International Journal of Environmental Sciences
ISSN: 2229-7359
Vol. 11 No. 4S, 2025
https://www.theaspd.com/ijes.php

Alginate-Modified Biochar Beads for Rhodamine B Removal: A Sustainable Approach to Water Pollution Control

M.Padmaja[1*], R.Pamila[2], A.Sujaatha[3], S.Bala Padmaja[4], Kotha Manasa[5]
[1] Department of Civil Engineering, Mahatma Gandhi Institute of Technology, Hyderabad, India
[2]Department of Civil Engineering, Sri Sairam Engineering College, Chennai, India
[3]Department of Civil Engineering, Sri Sairam Engineering College, Chennai, India
[4] Department of Civil Engineering, Mahatma Gandhi Institute of Technology, Hyderabad, India
[5] Department of Civil Engineering, Chaitanya Bharathi Institute of Technology, Hyderabad, India

ABSTRACT
The growing demand for textiles has increased textile manufacturing, especially in developing countries, leading to severe environmental impacts from contaminated effluents. This study examined the adsorptive removal of Rhodamine B (RB) dye from aqueous solution using alginate-modified biochar beads (ALPPC, ALBPC, and ALPJC) derived from agricultural biomass: pumpkin peel (Cucurbita pepo L), plantain flower bracts (Musa acuminata), and mesquite tree bark (Prosopis juliflora). Biochar beads were prepared through ionic polymerization and characterized using SEM, FTIR, and BET analyses. Continuous mode adsorption experiments in a packed bed column system evaluated the effects of bed depth, flow rate, and influent concentration on breakthrough capacities and removal efficiency. The optimal column adsorption parameters for highest RB removal were: initial concentration 100 mg/L, flow rate 2 mL/min, and bed height 6 cm. The breakthrough curve was analyzed using Thomas and Yoon-Nelson models, with the latter closely agreeing with experimental data. Adsorption effectiveness followed the order ALPJC > ALPPC > ALBPC. The results show the potential of alginate-modified biochar composites as effective, eco-friendly, and low-cost adsorbents for treating dye-containing effluents, contributing to sustainable development goals (SDGs) by addressing rural livelihoods, converting waste to energy, and protecting water bodies' aesthetic appearance.
Keywords: Water pollution, Emission control, Textile dyestuff, Rhodamine B, Biochar, Adsorption, Packed bed column, Breakthrough curve, Sustainable development goals

1. INTRODUCTION

The increased demand for textile materials has led to growth in textile manufacturers, particularly in developing countries, severely impacting the environment due to contaminated effluents (Yaseen and Scholz 2021). The global annual production of dyes and pigments is approximately 7 × 107 tons, with the textile industry utilizing about 10,000 tons (Al-Tohamy et al. 2022). Color plays an attractive role in many fields, with industries using colored pigments to increase product aesthetics. However, their toxic nature poses significant risks to humans and the environment. It affects aquatic systems by causing eutrophication, impacting photosynthetic activity, depleting dissolved oxygen (Ramesh et al. 2021), and altering physicochemical and biological characteristics of water bodies. It may harm humans, affecting kidneys, reproductive system, liver, brain, and central nervous system (Hama Aziz et al., 2023). Dye toxicity inhibits soil microorganisms, reducing agricultural production (Methneni et al. 2021). Thus, removing hazardous color compounds from wastewater before disposal is essential. Effective techniques include chemical precipitation (Palansooriya et al., 2019), Advanced oxidation (Yuan et al.2021; Pandis et al.2022), photochemical degradation (Das et al., 2024), membrane filtration (Marszałek and Zyłła

[1] *Corresponding Author E-mail:* padmajamegham@gmail.com
Contact number: +91 9962433838
Orcid ID: 0000-0001-7371-2760

2021), biological treatment (Bhatia et al. 2017), and adsorption onto activated carbon (Hamad and Idrus 2022).

Compared with conventional methods, adsorption is favorable, eco-friendly, economical, and sustainable for removing pollutants. Activated carbon is preferred for eliminating pollutants from wastewater (Ezugbe and Rathilal, 2020). Due to the high costs of commercial activated carbon for dye adsorption, research on alternative adsorbents has intensified. A low-cost adsorbent requires minimal processing, is abundant, or is a byproduct from other industries. Some industrial and agricultural waste products, natural materials, and biosorbents may serve as cost-effective alternative sorbents.

Many have been tested for dye adsorption (Bailey et al.2019), including clay minerals (Ngulube et al.2017; Ewis et al.2022), industrial waste residues (Piaskowski et al. 2018; Ghime and Ghosh (2020), sugarcane dust (Ghernaout et al.2020), kenaf fibre char (Tang 2021), sewage sludge (Latha et al.2017), acid modified watermelon rinds (Husein et al., 2017) , orange peels (Khalfaoui et al., 2024), and cassava peels and roots (De Gisi et al. 2017). Recently, research has focused on biochar as an alternative to commercial activated carbon due to its good fixed carbon content and highly porous structure; it also helps reduce greenhouse gas emissions (Mosa et al., 2023). Biochar is reported as a potential low-cost adsorbent compared to activated carbon (Pamila et al. 2021). Additionally, using invasive plants as precursors for biochar production can improve their management and protect the environment (Das et al., 2020). Most adsorption experiments use powdered adsorbent materials.

However, due to reduced particle size, poor stiffness, low density, and weak mechanical strength, it is not viable for large-scale dye removal processes. Separating the adsorbent becomes difficult, causing loss after regeneration. Immobilizing the adsorbent in a polymeric matrix could solve these issues (Abdul Mubarak et al., 2020). In this study, biochar powder was modified into alginate-modified biochar beads through ionic polymerization and used for Rhodamine B (RB) remediation.

2. MATERIAL AND METHODS

2.1 Preparation of adsorbate solution

Stock solutions of basic cationic dyes selected for this study were prepared at a concentration of 1000 mg/L by dissolving the requisite quantity of dye powder in deionized water and subsequently diluting the solution to the desired concentrations.

Table 1 Characteristics of Rhodamine B

Molecular Formula	$C_{28}H_{31}N_2O_3Cl$
Molecular weight (g/mol)	479
C.I Name	Acid Red 52
C.I Number	45170
Maximum wavelength (λmax) (nm)	554

The solution pH was adjusted to the required level using 0.1M HCl and 0.1M NaOH. The characteristics and chemical structures of the dyes are presented in Table 1 and Figure 1, respectively.

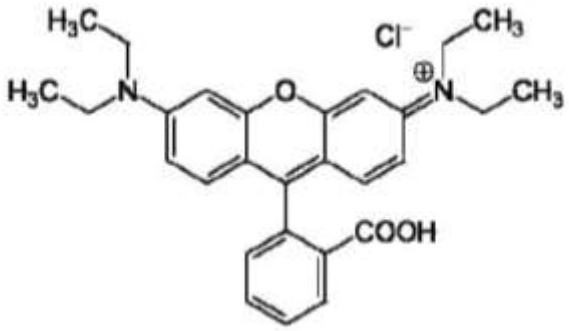

Fig.1 Structure of Rhodamine B

2.2 Selection and preparation of raw adsorbents from feedstock

For the production of biochar, three different agricultural waste materials were chosen: Prosopis juliflora (mesquite tree) bark, Musa acuminata species (plantain flower) bracts, and Cucurbita pepo L. (pumpkin peels). We purchased the Prosopis juliflora bark, pumpkin peels, and plantain flower bracts from nearby markets. Before being used further, all of the materials described above were cleaned with distilled water to get rid of contaminants and dirt particles. They were then sun-dried and then oven-dried at 110°C.

2.3 Preparation of biochar from Pumpkin peel (PPC), Bracts of plantain flower (BPC) and *Prosopis juliflora* bark (PJC)

Acid activation was performed using conventional protocols to enhance the effectiveness of raw pumpkin peel and plantain flower bracts. The raw PPC and BPC adsorbents were submerged in 18N sulfuric acid until completely charred, then heated and allowed to evolve fumes. The carbonized materials were rinsed with distilled water until neutrality, sun-dried, and heated for an hour at 350°C in a tube furnace. The heating rate was 5°C per minute. After pulverization and sieving to 200–300 μm, the biochar samples were designated PPC and BPC for further tests. Similarly, raw Prosopis juliflora bark adsorbents were immersed in sulfuric acid and prepared until complete charring occurred. The mixture was comminuted using a domestic grinder. The dried sample was heated in a tubular furnace under nitrogen atmosphere at 600°C for an hour, with a heating rate of 5°C/min. The biochar was cooled to room temperature, ground, and sieved to 200–300 μm, labeled as PJC, and used for further studies.

2.4 Preparation of alginate-modified biochar beads (ALPPC, ALBPC, ALPJC)

For preparing alginate-modified biochar beads, one part sodium alginate powder was placed in a 250 mL conical flask with 100 mL double-distilled water and agitated using a magnetic stirrer (REMI make) until a viscous gelatinous solution formed. Then, 1 part biochar (PJC, PPC, and BPC) was added and stirred until a homogeneous gel formed (Kumar et al. 2013). The gel was introduced dropwise into a calcium chloride solution and left for 3 h. The excess solution was rinsed with double distilled water, air-dried, subjected to hot air oven treatment, and designated as ALPJC, ALPPC, and ALBPC. Images of the alginate biochar beads are shown in Figure 2 a), b), and c).

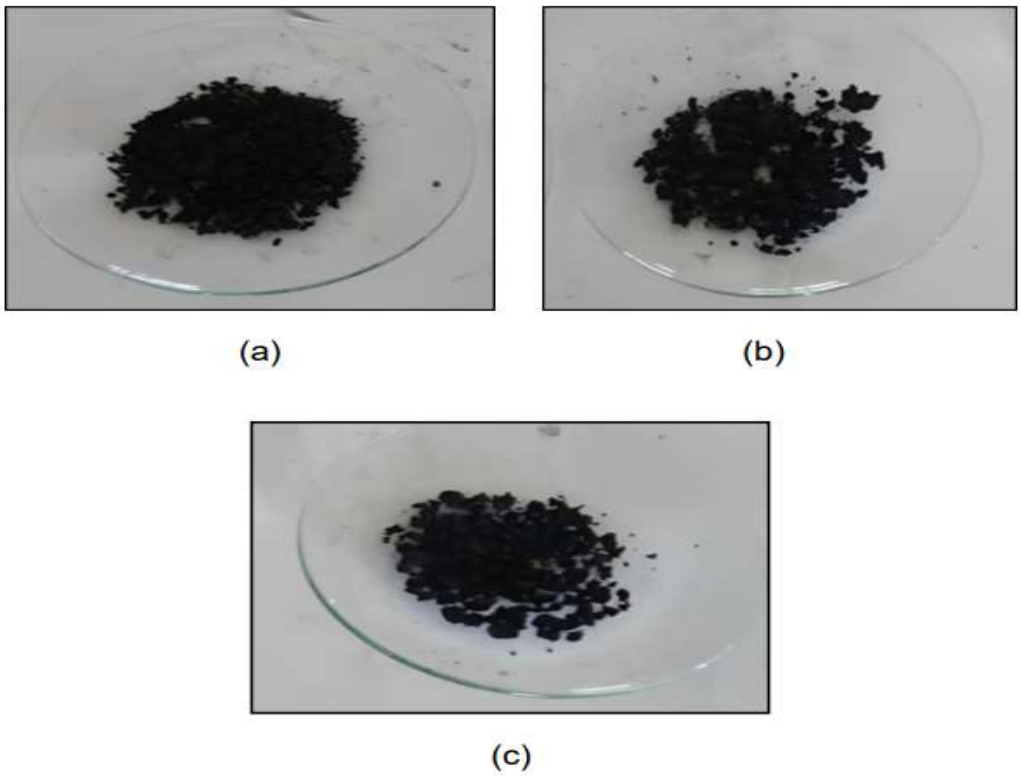

Fig. 2 Images of (a) ALPPC (b) ALBPC and (c) ALPJC

2.5 Adsorbents Characterization

Characterization studies are crucial to evaluate adsorbents' surface shape and physicochemical characteristics. Surface area characteristics were measured using a surface area analyzer (BELSORP mini II). The Brunauer-Emmett-Teller (BET) equation was used to measure the adsorbent samples' surface area using N2 adsorption-desorption after preheating between 200°C and 300°C. The adsorbents' surface area was expressed as m2/g. Scanning Electron Microscopy (SEM) analysis visualized constituents before and after adsorption, and the surface shape and microstructure of adsorbents. Samples were coated with a thin gold film before analysis. The JSM - 5610LV (JEOL - JAPAN) SEM examined the adsorbents' morphological characteristics. Fourier Transform Infrared (FTIR) spectroscopy analyzed the functional groups responsible for adsorption and surface functionalities. Adsorbent samples were prepared into translucent discs using KBr pellets. FTIR analysis using a Perkin Elmer spectrometer was performed in the 400 cm-1–4000 cm-1 wavelength range.

2.6 Column adsorption studies

Batch mode studies assessed adsorbents' capacity to eliminate pollutants at the laboratory-scale level. However, for practical applications, continuous-mode studies are necessary due to insufficient retention time. Packed bed fixed columns are more suitable for industrial applications to conduct adsorption experiments in a continuous process, as adsorbents maintain prolonged contact with wastewater in columns. Continuous mode adsorption studies for RB dye removal were conducted in a glass column (2.5 cm diameter, 18 cm length; Figure 3) packed with specific amounts of adsorbents for bed heights of 2cm, 4.5cm, and 6cm. Flow rates ranged from 2 ml/min, 4 ml/min, and 6 ml/min with inlet concentrations of 100 mg/L, 200 mg/L, and 300 mg/L. The dye solution was propelled upward into the column using a peristaltic pump and flowed through the sorbent bed where sorption occurred. Samples exiting the column were collected at regular intervals and analyzed for dye concentration using a UV-visible Spectrophotometer at a maximum wavelength (λmax) of 554 nm.

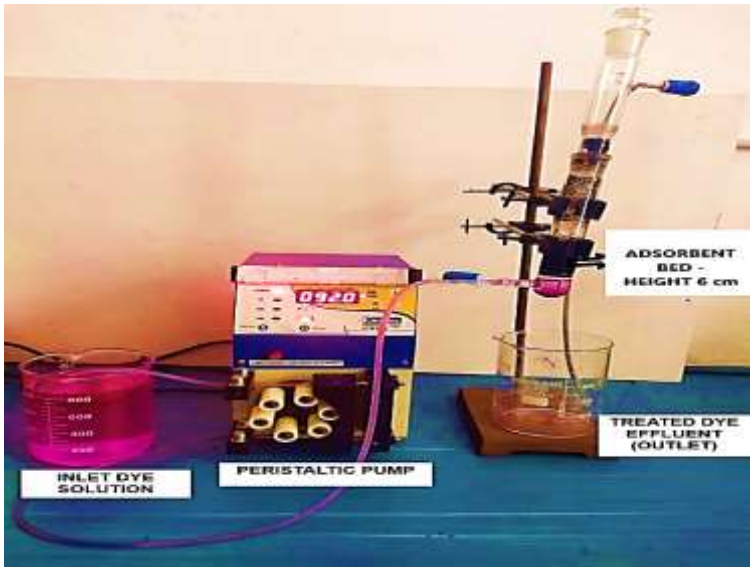

Fig. 3 Packed Bed Column

2.7 Column Breakthrough Curves

The efficiency of the packed bed column was obtained by drawing breakthrough curves. The duration and shape of the resultant breakthrough curve are critical in influencing the adsorption process and the dynamic responsiveness of a fixed-bed column for dye removal. The breakthrough curves are plots of Ct/Co versus time. The total volume of effluent ($V_{effluent}$) is calculated using the equation below,

$$V_{effluent} = Q.\ t_{total}$$

where, total is the total flow time (min) and Q is the flow rate (mL/min). The total amount of dye adsorbed (q_{total}) is calculated by integrating the product of the area (A) under the breakthrough curve and its rate of flow using the below equation,

$$q_{total} = \frac{QA}{1000} = \frac{Q}{1000}\int_{t=0}^{t=total} C_{ad}.dt$$

where, Q is the flow rate of the feed (mL/min), Cad is the concentration of dye adsorbed at a given time t. The total quantity of dye (m_{total}) fed to the column is calculated as

$$m_{total} = \frac{C_0\ Q\ t_{total}}{1000}$$

where, Co is the initial concentration of the dye in (mg/L), Q is the flow rate of the feed (mL/min), t_{total} is the total flow time (min). The total removal % is obtained from the below equation

$$\text{Total Removal}\ (\%) = \frac{q_{total}}{m_{total}} \times 100$$

In the above equation, q_{total} is the total amount of dye adsorbed and m_{total} is the total quantity of dye fed to the column

2.8 Column Adsorption Modelling Studies

Experimental data obtained from laboratory-scale column investigations were used to analyze the behavior of continuous-mode adsorption processes. To assess the efficacy and application of column settings for large-scale activities, a number of mathematical models have been created. The breakthrough curves observed for different flow rates, bed heights, and inlet dye concentrations were

predicted using the Thomas and Y-N models, which were used in this experiment to examine the column performance.

2.8.1 Thomas model

The Thomas model in its linearised form is given below

$$ln\left(\frac{C_o}{C_t} - 1\right) = \frac{K_{th} q_o X}{Q} - \frac{K_{th} C_o}{Q} V_{eff}$$

where, Q refers to flow rate of the effluent (mL/min), C_o is the concentration at inlet (mg/L), C_t is the outlet concentration (mg/L), q_o is the maximum uptake capacity (mg/g), X refers to the mass of the adsorbent (g), V_{eff} is the volume of the effluent (mL), K_{th} is the Thomas constant. The K_{th} and q_o values are derived from the slope & intercept of $[(C_o/C_t) - 1]$ vs V_{eff} plot.

2.8.2 Yoon - Nelson (Y-N) model

The Yoon - Nelson model in its linearised form is given below

$$ln\left(\frac{C_o}{C_o - C_t}\right) = K_{YN}\, t - \tau\, K_{YN}$$

where, C_o & C_t are the concentrations of the inlet and effluent, k_{YN} is the Y-N constant (min^{-1}), τ is the time for 50% breakthrough (minutes) and t is the time for breakthrough of the sample in minutes. The values of k_{YN} and τ can be obtained from the slope and intercept of ln $(C_t/C_o\text{-}C_t)$ vs t plot.

2.9 Desorption and Regeneration Studies

The ability of the prepared adsorbents to be reused was evaluated by performing desorption-regeneration studies. Many elutants, namely 0.1 M HCl, NaOH, Na_2CO_3 and EDTA, were used to desorb the pollutants from the loaded adsorbents. Each of the spent biosorbents was placed in 250 mL Erlenmeyer flasks, allowed to contact 100 mL of each elutant, and agitated for 120 min at 150 rpm. The decanted solution was centrifuged at 2000 rpm for 10 min, and the concentration of the supernatant was spectrophotometrically determined. After desorption, the pollutant-free adsorbents were thoroughly cleaned with water and subjected to adsorption analysis. The adsorption-desorption process was repeated several times until the efficiency was reduced.

3. RESULTS AND DISCUSSION

3.1 Characterization of alginate-modified biochar composite beads (ALPPC, ALBPC, ALPJC)

Figure 4(a), (b), and (c) show SEM images of the alginate-modified biochar composite beads ALPPC, ALBPC, and ALPJC, respectively.

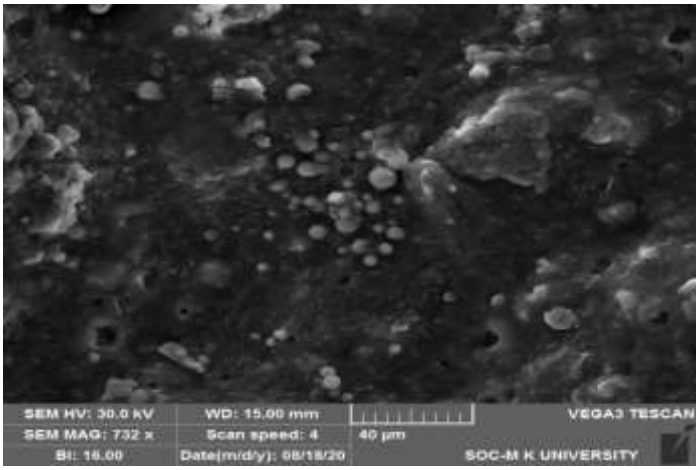

Fig. 4(a) SEM image of ALPPC

In general, all the surfaces of the alginate-modified biochar samples were found to be slightly smooth, with cracks formed owing to the swelling action of alginate, which resulted in an increase in the surface area, which facilitated the binding of cations from the aqueous solution.

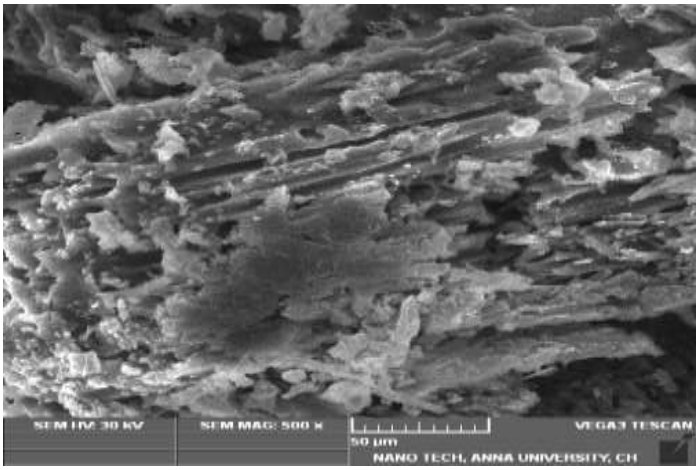

Fig. 4(b) SEM image of ALBPC

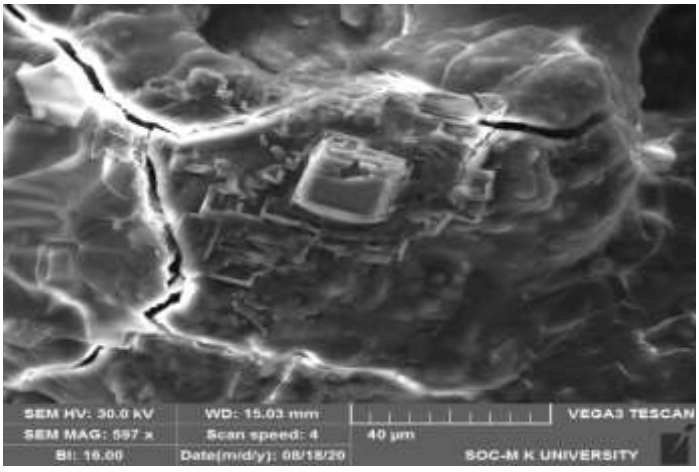

Fig. 4(c) SEM image of ALPJC

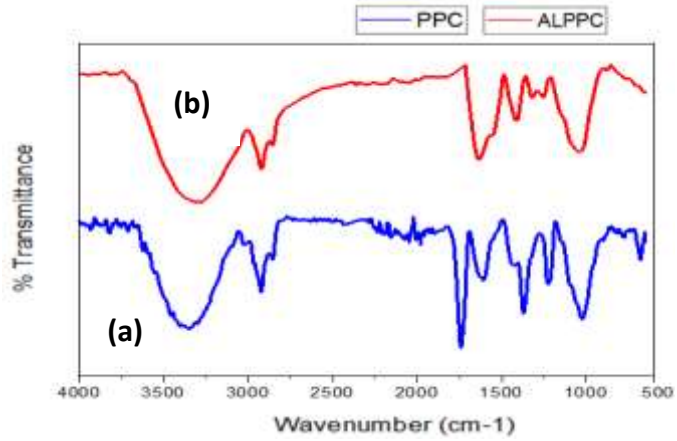

Fig. 5 FTIR images of (a) PPC & (b) ALPPC

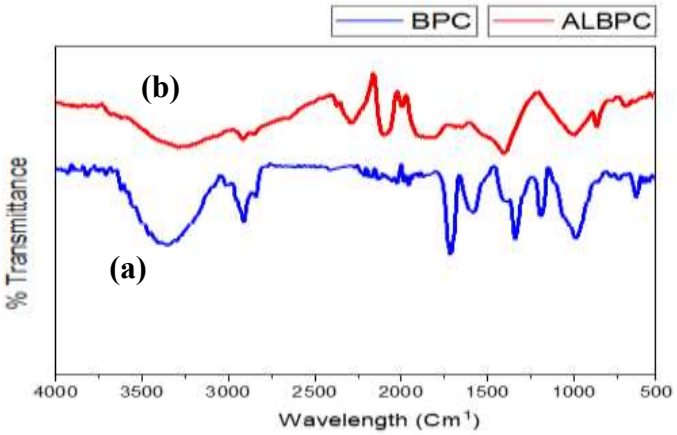

Fig. 6 FTIR images of (a) BPC & (b) ALBPC

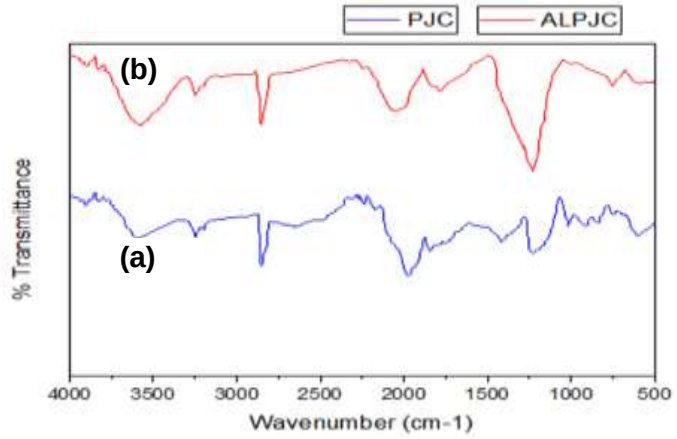

Fig. 7 FTIR images of (a) PJC & (b) ALPJC

To understand the changes in the functional groups of the raw biochar and alginate-modified biochar composites, the FT-IR spectra are illustrated in Figure 5a) and b). Figure 5a) shows the FTIR Spectrum of PPC, indicating several adsorption peaks. The broad peak at 3388.32 cm-1 was due to the (O-H) hydroxyl group. Peaks in the range of 2919.7 cm-1 to 2851.24 cm-1 represent symmetric or asymmetric C-H bond stretching of methyl groups. Peaks at 1698.02 cm-1, 1608.34 cm-1 and 1408.75 cm-1 represent C=O stretching of carboxylic acid and ester bonds. Peaks at 1251.58 cm-1, 1094.4 cm-1 and 612.9 cm-1 represent stretching of ionic and carboxylic groups. The FTIR spectrum of ALPPC, shown in Figure 5 b),

displays prominent peaks at 3230 cm-1, 2924.26 cm-1, 1625 cm-1 and 1024 cm-1. The shift in wave numbers and appearance of new peaks confirmed the existence of several functional groups and proper bonding between the biochar and alginate.

Figure 6 a) shows the FTIR spectrum of BPC. The peak at 3356 cm-1 represents O-H group stretching. Peaks at 2926.45 cm-1 indicate methyl group stretching, and symmetric carboxylic group (-COO) stretching vibrations appear at 1575.56 cm-1. The peak at 1373.07 cm-1 represents symmetrical stretching of -COO pectin, while the peak at 1114.65 cm-1 is attributed to alcohol and acid stretching vibrations. The peak at 768.49 cm-1 is due to C-H stretching of Alkynes and Aryl groups. Figure 6 b) shows -OH group stretching and additional peaks from carboxylic group interaction with sodium alginate. Figure 7a) shows the FTIR spectrum of PJC, with peaks at 3387 cm-1, 2924.52 cm-1, 2318.98 cm-1, 2110.71 cm-1, 1987.29 cm-1 and 1371.14 cm-1. Figure 7 b) shows the FTIR Spectrum of ALPJC, with a broad band at 3350.71 cm-1 from C-H stretching of hydroxyl, aliphatic, and amine groups. These groups enable electrostatic interactions between dye molecules and adsorbents. Figure 7 b) provides evidence for -OH bond stretching at 3412 cm-1, 2724.74 cm-1, 1417.44 cm-1, 1370 cm-1, 1022 cm-1, 717.23 cm-1, confirming various functional groups on ALPJC's surface.

The Brunauer-Emmet-Teller (BET) surface area analysis results showed that the surface area of alginate-modified biochar is 6.82 m^2/g, 6.13 m^2/g and 8.19 m^2/g for ALPPC, ALBPC and ALPJC, respectively. The surface area increased due to alginate polymer deposition on the biochar surface (Negrea et al.2020). The mean pore diameter of alginate-modified biochar is 19.04 nm, 26.12 nm and 16.32 nm for ALPPC, ALBPC and ALPJC respectively, indicating mesoporous adsorbents. The total pore volume of alginate-modified biochar is 0.106 cm^3/g, 0.094 cm^3/g and 0.073 cm^3/g for ALPJC, ALPPC and ALBJC, respectively.

3.2 Column adsorption studies

Continuous mode studies are essential for real-time applications. A packed-bed fixed column is an efficient method for cyclic sorption-desorption in process applications. Furthermore, the packed column offers various intrinsic advantages, such as ease of operation, cost-effectiveness, and precise adaptation to real-world wastewater systems. Continuous mode adsorption studies for the removal of RB dyes were conducted in a glass column 2.5 cm in diameter and 18 cm in length, and the selected adsorbents were loaded into the column to achieve the required bed heights. A peristaltic pump was used to force the dye solution into the column and allow it to run through the sorbent bed where sorption occurred. The samples flowing through and exiting the top of the column were collected and tested for the dye concentration. The effects of the bed height (2, 4.5, and 6 cm), flow rate (2, 4, and 6 mL/min), and inlet dye concentration (100, 200, and 300 mg/L) were studied, and breakthrough curves were obtained (Sazali et al. 2020). The data in the column were analyzed using the Thomas and Yoon–Nelson models to interpret the effects of each parameter.

3.2.1 Influence of bed height on RB adsorption

The influence of adsorbent bed height on the removal efficiency of the biochar adsorbents towards RB dye was initially investigated by increasing the bed height from 2 cm to 6 cm, while constantly maintaining the dye concentration at 100 mg/L and the rate of flow at 2 mL/min. It was observed from Figure 8 that S-shaped break-through curves were obtained for all depths but the slope of the break-through curves declined with the increase in bed depth, the steepness of the curve decreased with the increase in bed height. Breakthrough curves proved that as bed heights increased, correspondingly breakthrough and saturation times increased, this might be because of the presence of more binding sites on the adsorbent surface for the molecules. An increase in bed height leads to a decrease in axial depression which results in the diffusion of dye molecules into the surface of the adsorbent. More volume of effluent gets treated

at a longer saturation time. At 6 cm bed height, a high removal efficiency of 69.1% was reported for ALPJC and 64.7%, 62.4% for ALPPC, ALBPC respectively.

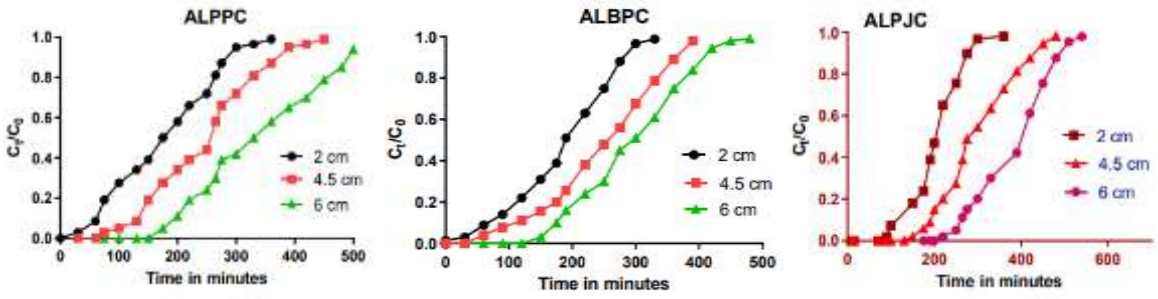

Fig. 8 Influence of bed height on RB adsorption

3.2.2 Influence of flow rate on RB adsorption

The influent flow rate is an important parameter for evaluating the effectiveness of adsorbents. In this study, different flow rates (2, 4.5, and 6 mL/min) were used to determine the effect of varying flow rates on the breakthrough curves (Figure 9) for RB adsorption onto the biochar adsorbents. Figure 8 shows that lower flow rates resulted in longer breakthrough and saturation times. At higher flow rates, the breakthrough point and saturation occurred quickly, and the adsorption capacity was reduced owing to the insufficient residence time of the solute in the column. Similar observations have been reported by several researchers (Chowdhury et al. 2020). An increase in the flow rate resulted in a shorter saturation time. The removal efficiency was maximum at 2 mL/min, with ALPJC exhibiting a high efficiency of 66.17% and ALPPC and ALBPC exhibiting efficiencies of 63.75% and 61.25%, respectively.

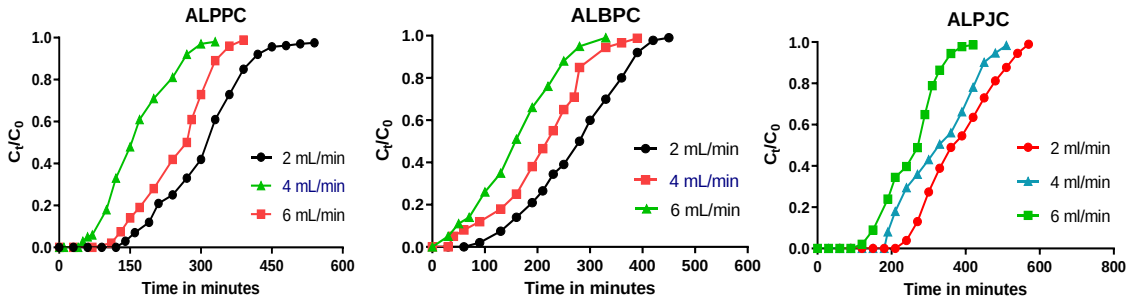

Fig. 9 Influence of Flow rate on RB adsorption

3.2.3 Influence of inlet concentration on RB adsorption

The influence of the inlet dye concentration on RB adsorption onto the biochar adsorbents was studied by varying it from 100 mg/L to 300 mg/L at a constant flow rate of 2 mL/min and a bed height of 6 cm, as shown by the breakthrough curve in Figure 10. At the highest concentration of 300 mg/L, the breakthrough curves became steeper, and the adsorbent bed tended to become saturated more quickly (Sivakumar and Palanisamy 2020). The breakthrough curves were flatter at lower concentrations, and a decrease in the initial MB concentration resulted in an extended breakthrough curve, indicating that a higher volume of the solution could be treated. At an inlet dye concentration of 100 mg/L, ALPJC exhibited a higher removal efficiency (67.7%) than ALPJC and ALBPC (65.5%, 63%, and 62.9%, respectively).

International Journal of Environmental Sciences
ISSN: 2229-7359
Vol. 11 No. 4S, 2025
https://www.theaspd.com/ijes.php

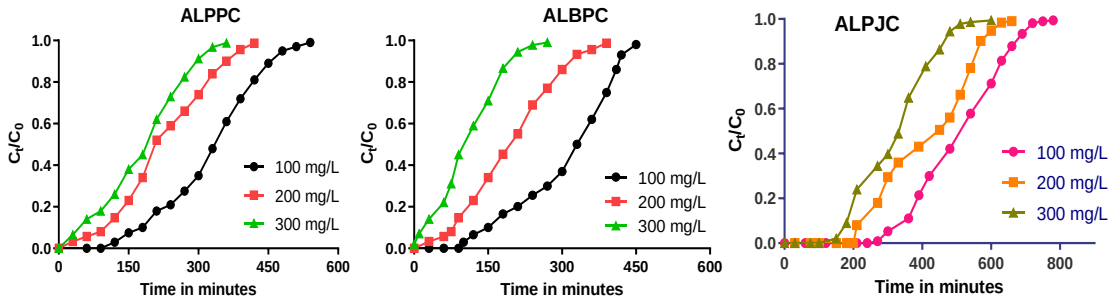

Fig. 10 Influence of inlet concentration on RB adsorption

3.3 Column kinetic study

Many mathematical models have been formulated to ascertain and predict the dynamic behavior of column beds. Two well-known and reliable models (Thomas model, Yoon model, and Nelson model) were used to analyze the column performance.

3.3.1 Thomas model

The Thomas model plots at variable bed height, flow rate, and inlet dye concentration are presented in Figure 11, Figure 12, and Figure 13, respectively.

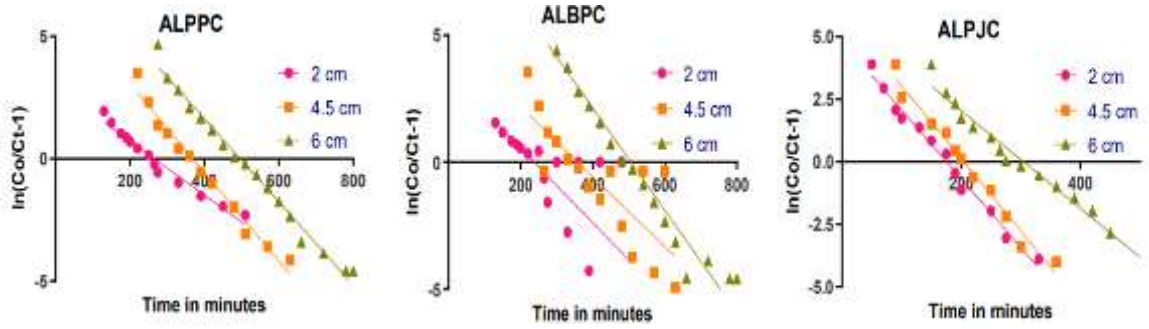

Fig. 11 Thomas model plots for RB adsorption – Influence of bed height

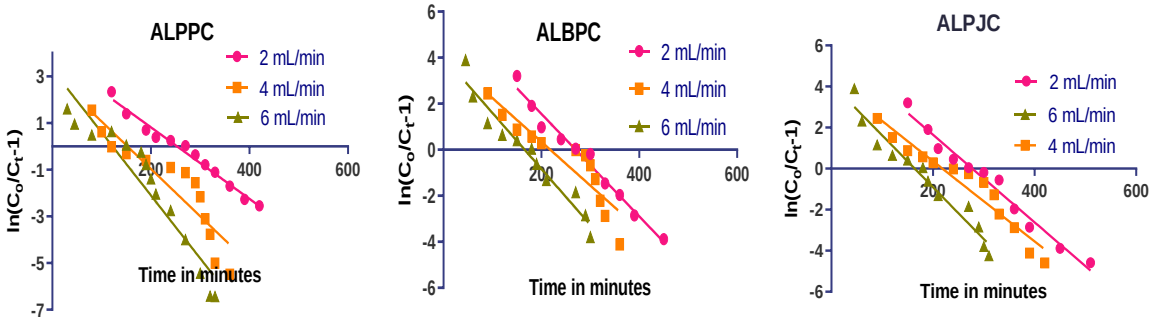

Fig. 12 Thomas model plots for RB adsorption – Influence of flow rate

International Journal of Environmental Sciences
ISSN: 2229-7359
Vol. 11 No. 4S, 2025
https://www.theaspd.com/ijes.php

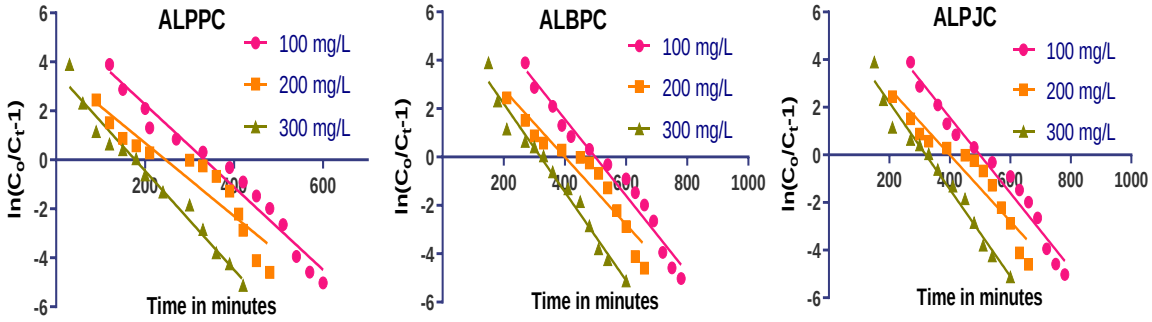

Fig. 13 Thomas model plots for RB adsorption – Influence of inlet dye concentration

It was observed that both the q_o (adsorption capacity) and Thomas constant K_{TH} values declined with an increase in the inlet dye concentration and flow rate. However, the values increased with an increase in the bed height. The Thomas model shows only a moderate fit to the experimental data, and is indicated by a low range of correlation coefficient values (R^2).

3.3.2 Yoon-Nelson (Y-N) model

The Y-N model was employed to determine its applicability for the column-mode adsorption study of RB dyes using biochar adsorbents. The Y-N plots for RB dye adsorption at various bed depths, flow rates, and inlet dye concentrations are shown in Figure 14, Figure 15 and Figure 16, respectively.

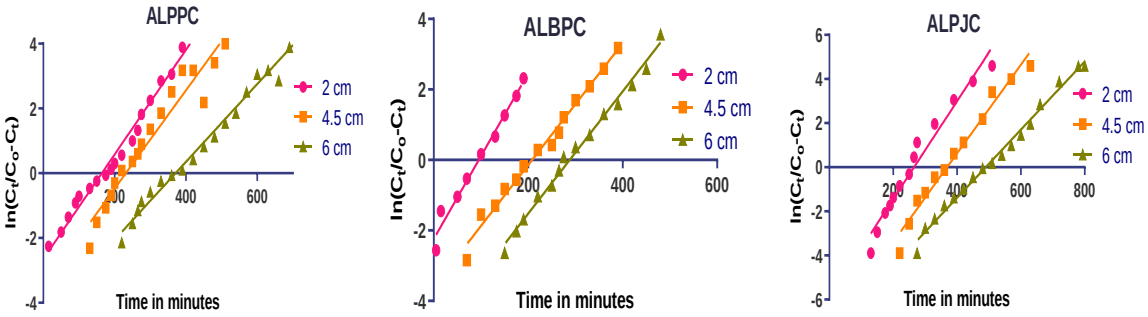

Fig. 14 Y-N model plots for RB adsorption – Influence of bed height

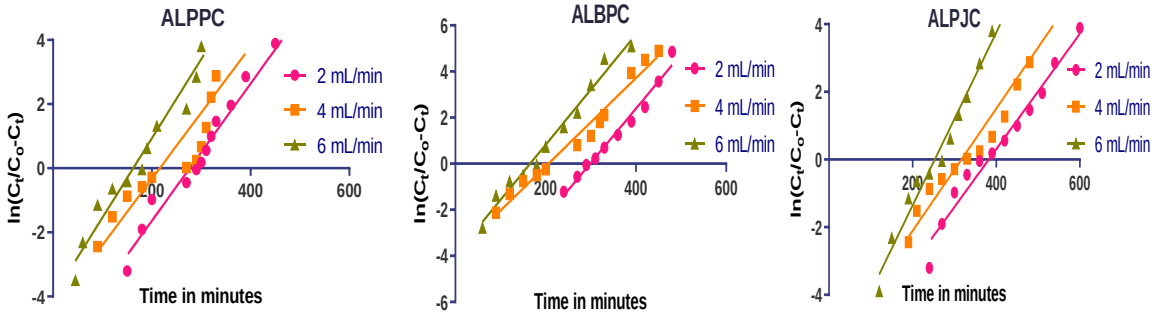

Fig. 15 Y-N model plots for RB adsorption – Influence of Flow rate

International Journal of Environmental Sciences
ISSN: 2229-7359
Vol. 11 No. 4S, 2025
https://www.theaspd.com/ijes.php

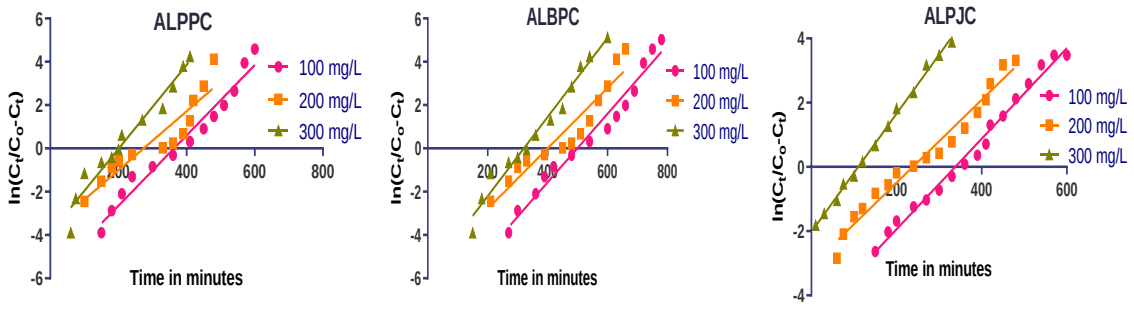

Fig. 16 Y-N model plots for RB adsorption – Influence of inlet concentration

It was observed that the Y-N constant K_{YN} increased with an increase in the bed height and inlet concentration but declined with an increase in the flow rate. It was observed that the τ values declined with an increase in the flow rate and inlet dye concentration, which could be due to the rapid saturation of the column at higher flow rates. However, it increased with increasing bed height as the accessibility of the adsorption sites increased. The Y-N model best suited the experimental data, with R^2 values between 0.889 and 0.993.

3.4 Desorption studies

To examine the possibility of reusing *the adsorbents* in the biosorption process, regeneration experiments were conducted for three repeated sorption-desorption cycles. To study the desorption efficiency of biochar, several elutants, such as HCl, H_2SO_4, HNO_3, NaOH, and deionized water, were examined for their potential to elute TB and RB dyes (Patel 2021).

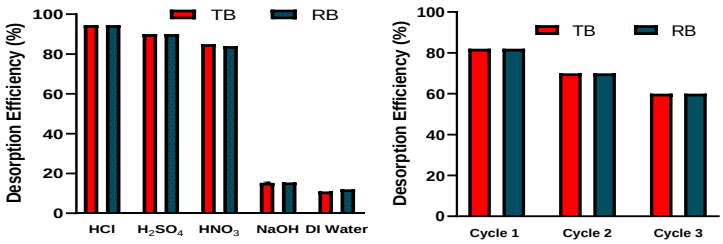

Fig. 17 Desorption potential of ALPPC on different elutants and Regeneration Cycles - ALPPC

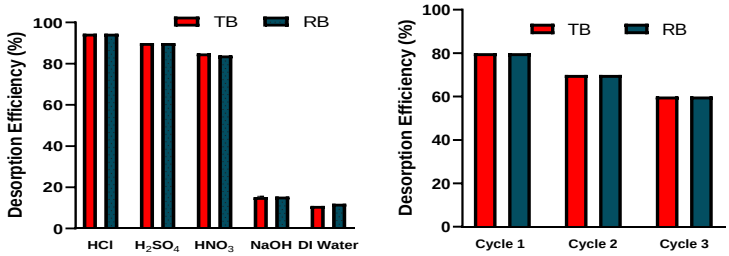

Fig. 18 Desorption potential of ALBPC on different elutants and Regeneration Cycles –ALBPC

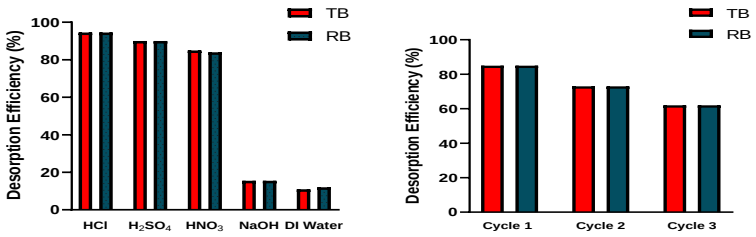

Fig. 19(a) Desorption potential of ALPJC on different elutants and Regeneration Cycles - ALPJC

Figure 17, Figure 18 and Figure 19 show the desorption efficiencies of different elutants on the adsorbents.

4. CONCLUSION

The present investigation showed that alginate-modified biochar beads prepared from three agricultural biomasses (pumpkin peel, plantain flower bracts, and mesquite tree bark) are promising adsorbents for Rhodamine B removal from aqueous solutions. Characterization processes highlighted the potential of biochar adsorbents, showing notable physicochemical attributes, extensive surface area, pore distribution, and functional groups crucial for efficient dye removal. Adsorption studies in column mode for all adsorbents indicated that dye removal efficiency, breakthrough time, volumetric efficiency, and exhaustion time increased with bed depth but declined with flow rate. Adsorption depended on bed depth, flow rate, and influent dye concentration. Experimental column adsorption data were fitted using Thomas and Y-N models. For the Thomas model, adsorption capacity q0 and constant KTH decreased with increasing inlet dye concentration and flow rate, while increasing bed height increased both q0 and KTH values. For the Yoon-Nelson model, constant KYN increased with bed height and inlet concentration but decreased with flow rate. τ values decreased with increased flow rate and inlet dye concentration. The Y-N model best fitted the experimental data, with correlation coefficients between 0.845-0.985. Results indicated that alginate composite beads derived from Prosopis juliflora (ALPJC) are promising for color removal from aqueous solutions. It is economically viable and abundantly available, making it suitable for treating dye-bearing wastewater. This can be further studied for real-time industrial wastewater treatment. Continuous mode studies revealed adsorption effectiveness in the order, ALPJC > ALPPC > ALBPC.

5. REFERENCES

Abdul Mubarak, N. S., Sabar, S., Khor, H. P., Wilson, L. D., Jawad, A. H., & Chuan, T. W. (2020). Immobilized Fe-Loaded Chitosan Film for Methyl Orange Dye Removal: Competitive Ions, Reusability, and Mechanism. *Journal of Polymers and the Environment*, *29*(4), 1050–1062. https://doi.org/10.1007/s10924-020-01949-8

Al-Tohamy R, Ali S S, Li F, Okasha K M, Mahmoud Y A G, Elsamahy T, Jiao H, Fu Y, and Sun J (2022) "A critical review on the treatment of dye-containing wastewater: Ecotoxicological and health concerns of textile dyes and possible remediation approaches for environmental safety", Ecotoxicology and Environmental Safety, Vol. 231, pp. 113160. https://doi.org/10.1016/j.ecoenv.2021.113160.

Bailey S.E., Olin T.J., Bricka R.M. and Adrian D.D, (2019) "A Review of Potentially Low-Cost Sorbents for Heavy Metals", Water Research, Vol. 33, pp. 2469-247.

Bhatia D., Sharma, N. R., Singh, J., and Kanwar R. S, (2017) "Biological methods for textile dye removal from wastewater: A review", Critical Reviews in Environmental Science and Technology, Vol. 47(19), pp. 1836 –1876

Chowdhury Z.Z., Zain S.M., Rashi, A.K., Rafique R F., and Khalid K, (2020) "Breakthrough Curve Analysis for Column Dynamics Sorption of Mn (II) Ions from Wastewater by Using Mangostana garcinia Peel-Based Granular-Activated Carbon," Journal of Chemistry, Vol.1(1), pp.1–8.

Das, M., Ghatak, A., Guha Ray, P., & Stachewicz, U. (2024). Advancements in ZnO-based photocatalysts for effective rhodamine dye removal from water. *Sustainable Materials and Technologies*, *42*, e01138. https://doi.org/10.1016/j.susmat.2024.e01138

Das, S. K., Avasthe, R., & Ghosh, G. K. (2020). Biochar application for environmental management and toxic pollutant remediation. *Biomass Conversion and Biorefinery*, *13*(1), 555–566. https://doi.org/10.1007/s13399-020-01078-1

Ewis D., Ba-Abbad M. M., Benamor A., and El-Naas M. H, (2022) "Adsorption of organic water pollutants by clays and clay minerals composites: A comprehensive review", Applied Clay Science, Vol. 229, pp. 106686.

Ezugbe E.O and Rathilal S, (2020) "Membrane Technologies in Wastewater Treatment: A Review", Membranes, Vol. 10(5), pp. 89.

Ghernaout D., Elboughdiri N., and Ghareba S, (2020) "Fenton Technology for Wastewater Treatment: Dares and Trends", Open Access Library, Vol. 07(01), pp.1-26.

Ghime D and Ghosh P, (2020) "Advanced Oxidation Processes: A Powerful Treatment Option for the Removal of Recalcitrant Organic Compounds", Advanced Oxidation Processes - Applications, Trends, and Prospects, IntechOpen.

Hama Aziz, K. H., Mustafa, F. S., Omer, K. M., Hama, S., Hamarawf, R. F., & Rahman, K. O. (2023). Heavy metal pollution in the aquatic environment: efficient and low-cost removal approaches to eliminate their toxicity: a review. *RSC Advances*, *13*(26), 17595–17610. https://doi.org/10.1039/d3ra00723e

Hamad H.N and Idrus S, (2022) "Recent Developments in the Application of Bio-Waste-Derived Adsorbents for the Removal of Methylene Blue from Wastewater: A Review" Polymers, Vol. 14 pp (4),783.

Husein, D. Z., Battia, M., & Aazam, E. (2017). Adsorption of Cadmium(II) onto Watermelon Rind Under Microwave Radiation and Application into Surface Water from Jeddah, Saudi Arabia. *Arabian Journal for Science and Engineering*, *42*(6), 2403–2415. https://doi.org/10.1007/s13369-016-2381-2

Khalfaoui, A., Panico, A., Hammoud, A., Benalia, A., Selama, Z., Derbal, K., & Pizzi, A. (2024). Removal of Chromium (VI) from Water Using Orange peel as the Biosorbent: Experimental, Modeling, and Kinetic Studies on Adsorption Isotherms and Chemical Structure. *Water*, *16*(5), 742. https://doi.org/10.3390/w16050742

Latha A., Partheeban P., and Ganesan R., (2017) "Treatment of Textile Wastewater by Electrochemical Method", International Journal of Earth Sciences and Engineering, Vol. 10(01), pp. 146–149.

Marszałek J and Zyłła R, (2021) "Recovery of Water from Textile Dyeing Using Membrane Filtration Processes," Processes, Vol. 9 (10), pp. 1833.

Methneni N, Morales-González J A, Jaziri A, Mansour H B, and Fernandez-Serrano M, (2021) "Persistent organic and inorganic pollutants in the effluents from the textile dyeing industries: Ecotoxicology appraisal via a battery of biotests" Environmental Research, Vol. 196, pp.110956.

Mosa, A., El Kenawy, A. M., Mansour, M. M., Soliman, E., El Alfy, M., & El-Ghamry, A. (2023). Biochar as a Soil Amendment for Restraining Greenhouse Gases Emission and Improving Soil Carbon Sink: Current Situation and Ways Forward. *Sustainability*, *15*(2), 1206. https://doi.org/10.3390/su15021206

Negrea A., Mihailescu M., Mosoarca G., Ciopec M., Duteanu N., Negrea P and Minzatu V, (2020) "Estimation on Fixed-Bed Column 147 Parameters of Breakthrough Behaviors for Gold Recovery by Adsorption onto Modified/Functionalized Amberlite XAD7," International Journal of Enviromental Research and Public Health, Vol.17(18), pp. 6868.

Ngulube T., Gumbo, J. R., Masindi, V., and Maity A, (2017) "An update on synthetic dyes adsorption onto clay-based minerals: A state-of-art review", Journal of Environmental Management, Vol.191, pp.35–57.

Palansooriya, K. N., Yang, Y., Tsang, Y. F., Sarkar, B., Hou, D., Cao, X., Meers, E., Rinklebe, J., Kim, K.-H., & Ok, Y. S. (2019). Occurrence of contaminants in drinking water sources and the potential of

biochar for water quality improvement: A review. *Critical Reviews in Environmental Science and Technology*, *50*(6), 549–611. https://doi.org/10.1080/10643389.2019.1629803

Pandis P. K., Kalogirou C., Kanellou E., Vaitsis C., Savvidou M. G., Sourkouni G., Zorpas A. A., and Argirusis C, (2022) "Key Points of Advanced Oxidation Processes (AOPs) for Wastewater, Organic Pollutants and Pharmaceutical Waste Treatment: A Mini Review", Chemical Engineering, Vol. 6(1), pp. 8. https://doi.org/10.3390/chemengineering6010008.

Patel H, (2021) "Review on solvent desorption study from exhausted Adsorbent", Journal of Saudi Chemical Society, Vol. 25(8), pp. 101302.

Piaskowski K., Świderska-Dąbrowska R., and Zarzycki P K, (2018) "Dye Removal from Water and Wastewater Using Various Physical, Chemical, and Biological Processes", Journal of AOAC International, Vol. 101(5), pp. 1371–1384.

Ramesh, P., Padmanabhan, V., Arunadevi, R., Sudha, P., El-Zaher M.A. Mustafa, A., Al-Ghamdi Ahmed, A., Alajmi, A. H., & Elshikh, M. S. (2021). Batch and column mode removal of the turquoise blue (TB) over bio-char based adsorbent from Prosopis Juliflora: Comparative study. Chemosphere, 271, 129426. https://doi.org/10.1016/j.chemosphere.2020.129426

Ramesh, P., Padmanabhan, V., Saravanan, P. et al. (2021) Batch studies of turquoise blue dye (TB) adsorption onto activated carbon prepared from low-cost adsorbents: an ANN approach. Biomass Conv. Bioref. 13, 3267–3280. https://doi.org/10.1007/s13399-021-01355-7.

Sazali N., Harun Z., and Sazali N, (2020) "A Review on Batch and Column Adsorption of Various Adsorbent Towards the Removal of Heavy Metal", Journal of Advanced Research in Fluid Mechanics and Thermal Sciences, Vol.67(2), pp 66-88.

Tang K H D, (2021) "Interactions of Microplastics with Persistent Organic Pollutants and the Ecotoxicological Effects: A Review", Tropical Aquatic and Soil Pollution, Vol. 1(1), pp. 24–34.

Yaseen DA and Scholz M (2021) "Textile dye wastewater characteristics and constituents of synthetic effluents: a critical review", International Journal of Environmental Science and Technology, Vol. 16, pp. 1193-1226, 201. https://doi.org/10.1080/21655979.2020.1863034.

Yuan D, Yang K, Pan, S., Xiang Y, Tang S, Huang L, Sun M, Zhang X, Jiao T, Zhang Q, and Li B, (2021) "Peracetic acid enhanced electrochemical advanced oxidation for organic pollutant elimination", Separation and Purification Technology, Vol.276, pp.119317. https://doi.org/10.3390/coatings12040466.

Data Access Statement

The authors declare that no funds, grants, or other support were received during the preparation of this manuscript.

Author Contributions Statement

R.Pamila and M.Padmaja collaboratively designed the study. M.Padmaja conducted the experiments, A.Sujaatha performed data analysis, and wrote the initial draft of the manuscript S.Bala Padmaja and Kotha Manasa contributed to experimental design, provided technical guidance, and assisted in data interpretation. All the authors contributed to manuscript revisions, approved the final version, and agree to be accountable for all aspects of the work.

Ethical approval and consent to participate:

The authors declare that they have no known competing financial interests or personal relationships that seem to affect the work reported in this article.

Consent for Publication:

We do not have any individual person's data in any form.

Competing interest:

The authors declare that they have no conflict of interest